

1. INTRODUCTION

In steel construction, identical elevations are often required for flanges of secondary beams and primary beams for architectural purposes. Thus, secondary beams are usually coped at the flanges to facilitate erection and to achieve a compact connection between the secondary beams and the primary beams, as shown in Fig. 1. From the structural performance perspective, however, the load carrying capacity of a coped beam is inevitably reduced due to the removed flange (Milek 1980), exposing the beam to the risk of failure, both globally and locally. When lateral-torsional buckling of a coped beam (Gupta 1984; Ibrahim 2015) is prevented effectively, local failure near the coped region (Yam 2014) may occur. Specifically, the potential local failure modes of the coped beam ends include local web buckling, block shear, flexural yielding and shear yielding.

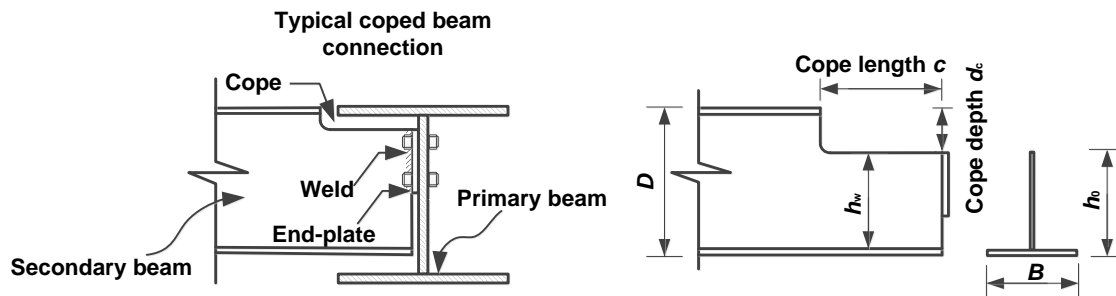


Fig. 1 Typical detail of a coped beam connection and symbols

Among these potential local failure modes of coped beams, local web buckling is one of the most common types. In fact, local web buckling failure raised concern among researchers since it was first observed in tests in late 1970s and early 1980s. In recent decades, some researchers have conducted investigations on the local web buckling behaviour of coped beams. For instance, a series of finite element (FE) analysis was first performed by Cheng (1984, 1986) to study the local buckling behaviour of top flange coped beams. Subsequently, Cheng (1986) developed a set of practical design equations for predicting the elastic local web buckling strength of coped beams based on a classical plate buckling model. From four more elastic local web buckling tests of coped beams and expanded FE analyses, Yam (2003) noticed that the buckling behaviour of the coped region might be governed by shear stress, particularly for specimens with a relatively small cope length to beam depth ratio. Therefore, an alternative calculation model was derived from the perspective of plate shear buckling, and practical design equations for quantifying the elastic local web buckling strength were constructed. More recently, Aalberg (2015) conducted an experimental study regarding the local web buckling resistance of top flange coped beams, and a simplified design formula for determining the load carrying capacity of coped beams was developed based on regression analyses. However, it should be noted that these research efforts on elastic local web buckling strength and behaviour of coped beams were primarily for hot-rolled sections with standard beam depth to web thickness ratio, whereas the available information on coped beams with slender web is quite limited. Even though two specimens with slender web were tested and analysed

in the research work of Cheng (1984), more efforts are still in need.

In this investigation, a finite element study was conducted to examine the local web buckling strength and behaviour of top flange coped beams with slender web. The developed models were compared with the test results of two specimens with slender web from Cheng (1984). Based on the validated models, a parametric study was then conducted, and effects of initial imperfections, web slenderness ratios, cope details (cope length to beam depth ratio and cope depth to beam depth ratio), and end-plate dimensions on the local web buckling strength and behaviour of coped beams with slender web were evaluated. To evaluate the applicability of current equations for predicting the local web buckling strength of coped beams with slender web, a comparison between the FE results and the local web buckling strength determined by the design equations was also made.

2. FINITE ELEMENT MODELLING OF SPECIMENS FROM THE LITERATURE

To have a better understanding of the strength and behaviour of coped beams with slender web, numerical models were developed and analysed using the FE method. The test results of two specimens with slender web from the literature (Cheng 1984) were used to validate the models. The details of these two specimens are presented in Table 1. The commercial FE analysis software ABAQUS (ABAQUS Version 6.12 (2012)) was used to perform the analyses. Measured dimensions of the specimens and the actual material properties obtained from coupon tests were employed in the models. Both the material and geometric nonlinearities were considered in the analyses, and the material nonlinearity for FE models was calibrated following the isotropic elastic-plastic trilinear law and the von Mises yield criterion. The entire coped beams were modelled using four-node, reduced integration, and finite strain shell elements (S4R element in ABAQUS), and the mesh in the coped region was refined. An overview of the FE model is presented in Fig. 2.

Table 1 Summary of the specimens with slender web (Cheng 1984)

No	Specimen code	D (mm)	B (mm)	t_w (mm)	t_f (mm)	h_w/t_w	d_c/D	c/D
1	PB26A	673.10	152.40	3.35	4.60	198	0.043	0.49
2	PB26B	673.10	152.40	3.35	4.60	198	0.034	0.31

To trigger the expected local web buckling failure or plate shear buckling failure near the cope for the specimens, initial imperfections were introduced in the analyses. The initial imperfection in terms of the first buckling shape was determined by an eigenvalue analysis, and then a scale factor was employed to adjust the peak value. In the analyses, the peak initial imperfection of 0.5 mm was used for specimen PB26A and PB26B, according to a trial-and-error procedure.

As for the boundary condition of the end-plate, an idealised boundary condition with translation displacement restraints at the bolt holes of the end-plate was first considered for simplification (Fig. 2). Also, boundary conditions with spring elements

